A FINITE ELEMENT METHOD FOR TWO-DIMENSIONAL LINEAR ELASTICITY

by Stephen V. Harren
http://www.harren.us

0. Contents

1. Governing Equations

The stress equilibrium equations are

$$\sigma_{ij,i} = 0\,, \tag{1.1}$$

where σ_{ij} is the stress tensor, which is the force intensity acting in the $j-$direction on an internal face whose normal is the $i-$direction. Also, herein, the comma denotes partial differentiation with respect to the spatial coordinates. The components of the strain tensor ε_{ij} are given by

$$\varepsilon_{ij} = \frac{1}{2}\left(u_{i,j} + u_{j,i}\right)\,, \tag{1.2}$$

where u_i is the displacement vector.

Hooke's Law is

$$\begin{aligned}
\sigma_{xx} &= \frac{1}{C(1-2\nu^*)}\left[\,(1-\nu^*)\varepsilon_{xx} + \nu^*\varepsilon_{yy}\,\right]\,,\\
\sigma_{yy} &= \frac{1}{C(1-2\nu^*)}\left[\,(1-\nu^*)\varepsilon_{yy} + \nu^*\varepsilon_{xx}\,\right]\,,\\
\sigma_{xy} &= \frac{1}{C}\,\varepsilon_{xy}\,,
\end{aligned} \tag{1.3}$$

or inversely

$$\varepsilon_{xx} = C\left[\,(1-\nu^*)\sigma_{xx} - \nu^*\sigma_{yy}\,\right]\,, \qquad \varepsilon_{yy} = C\left[\,(1-\nu^*)\sigma_{yy} - \nu^*\sigma_{xx}\,\right]\,, \qquad \varepsilon_{xy} = C\sigma_{xy}\,, \tag{1.4}$$

where

$$C = \frac{1+\nu}{E}\,, \quad \nu^* = \nu \ \text{(plane strain)}\,, \quad \nu^* = \frac{\nu}{1+\nu} \ \text{(plane stress)}. \tag{1.5}$$

In eqns. (1.5), E is Young's modulus and ν is Poisson's ratio. Also,

$$\begin{aligned}
&\text{plane strain:} \quad \varepsilon_{zz} = 0\,, \quad \sigma_{zz} = \nu\left(\sigma_{xx} + \sigma_{yy}\right)\\
&\text{plane stress:} \quad \sigma_{zz} = 0\,, \quad \varepsilon_{zz} = -\frac{\nu}{1-\nu}\left(\varepsilon_{xx} + \varepsilon_{yy}\right)
\end{aligned}\,. \tag{1.6}$$

Finally, eqns. (1.3) may be written in tensorial form as

$$\sigma_{ij} = L_{ijkl}\varepsilon_{kl}\,, \qquad L_{ijkl} = \frac{1}{C}\left[\,I_{ijkl} + \frac{\nu^*}{1-2\nu^*}\delta_{ij}\delta_{kl}\,\right]\,, \qquad I_{ijkl} = \frac{1}{2}\left(\delta_{ik}\delta_{jl} + \delta_{jk}\delta_{il}\right)\,, \tag{1.7}$$

where δ_{ij} is the two-dimensional identity matrix (or Kronecker delta).

In polar coordinates, the stress equilibrium equations (1.1) are

$$\sigma_{rr,r} + \frac{1}{r}\sigma_{r\theta,\theta} + \frac{1}{r}(\sigma_{rr} - \sigma_{\theta\theta}) = 0\,, \qquad \sigma_{r\theta,r} + \frac{1}{r}\sigma_{\theta\theta,\theta} + \frac{2}{r}\sigma_{r\theta} = 0\,. \tag{1.8}$$

Hooke's Law in polar coordinates is the same as eqns. (1.3): just make the replacements $x \to r$ and $y \to \theta$. In polar coordinates the strain-displacement relations (1.2) are

$$\varepsilon_{rr} = u_{r,r}\,, \qquad \varepsilon_{\theta\theta} = \frac{1}{r}u_{\theta,\theta} + \frac{1}{r}u_r\,, \qquad \varepsilon_{r\theta} = \frac{1}{2}\left(\frac{1}{r}u_{r,\theta} + u_{\theta,r} - \frac{1}{r}u_\theta\right)\,. \tag{1.9}$$

2. Principle of Virtual Work

Multiply the equilibrium equation (1.1) by a once differentiable vector field u_j^* (the so-called virtual displacement) to obtain

$$u_j^* \sigma_{ij,i} = 0 \,. \tag{2.1}$$

By the product rule of differentiation $\left(u_j^* \sigma_{ij}\right)_{,i} = u_{j,i}^* \sigma_{ij} + u_j^* \sigma_{ij,i}$, which when put into eqn. (2.1) yields

$$u_{j,i}^* \sigma_{ij} = \left(u_j^* \sigma_{ij}\right)_{,i} \,. \tag{2.2}$$

Next, by using Hooke's Law (1.7) and the symmetries of L_{ijkl}, eqn. (2.2) is

$$u_{j,i}^* L_{ijkl} u_{l,k} = \left(u_j^* \sigma_{ij}\right)_{,i} \,. \tag{2.3}$$

Now, integrate eqn. (2.3) over the domain A and use the Divergence Theorem to see

$$\int_A u_{j,i}^* L_{ijkl} u_{l,k} \, \mathrm{d}A = \oint_t u_j^* T_j \, \mathrm{d}t \,, \tag{2.4}$$

which is the Principle of Virtual Work. In eqn. (2.4), t is the coordinate around the boundary of A, and $T_j = n_i \sigma_{ij}$ is the traction vector acting on the boundary (**n** is the outward-pointing unit normal vector on the boundary). Finally, as seen from eqn. (2.4), admissible boundary conditions for linear elasticity are to prescribe either the displacement u_i or traction T_i at each point on the boundary.

3. Analytical Example in Cartesian Coordinates

Consider the stress field

$$\sigma_{xx} = \frac{12V}{H^3}(L-x)y \,, \qquad \sigma_{yy} = 0 \,, \qquad \sigma_{xy} = \frac{3V}{2H^3}(4y^2 - H^2) \,, \tag{3.1}$$

which spans the rectangular domain (a cantilever beam) of Fig. 1 below. Note that

$$\int_{-H/2}^{H/2} \sigma_{xy}(L,y)\mathrm{d}y = -V \,, \qquad \int_{-H/2}^{H/2} y\sigma_{xx}(0,y)\mathrm{d}y = VL \,, \tag{3.2}$$

so that $V > 0$ is the net shear force applied to the ends of the beam, and a moment VL is applied to the left end of the beam. Also, eqns. (3.1) satisfy the equilibrium eqns. (1.1) identically. With eqns. (3.1) and Hooke's Law (1.4), the strain components are

$$\varepsilon_{xx} = \frac{12VC(1-\nu^*)}{H^3}(L-x)y \,,$$
$$\varepsilon_{yy} = -\frac{12VC\nu^*}{H^3}(L-x)y \,, \tag{3.3}$$
$$\varepsilon_{xy} = \frac{3VC}{2H^2}(4y^2 - H^2) \,.$$

Finally, integrating the strains (3.3), via eqns. (1.2), such that

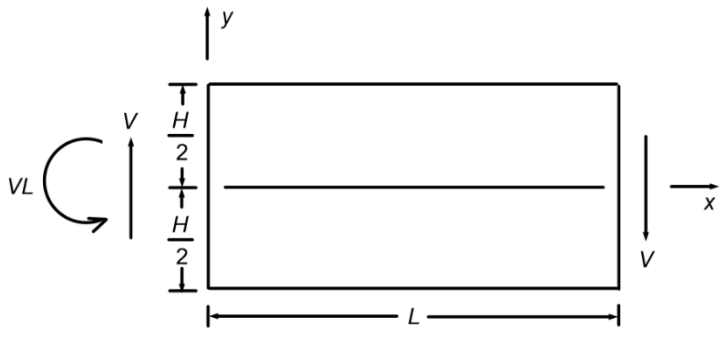

Figure 1. Domain of a cantilever beam.

$u_x(0,0) = u_y(0,0) = 0$ and $u_x(0, H/2) = 0$, one obtains the displacement field

$$u_x = \frac{VC}{2H^3}\,[\,12(1-\nu^*)(2Lx - x^2)y + 4(2-\nu^*)y^3 - (2-\nu^*)H^2 y\,]\,,$$
$$u_y = -\frac{VC}{2H^3}\,[\,12\nu^*(L-x)y^2 + 4(1-\nu^*)(3Lx^2 - x^3) + (4+\nu^*)H^2 x\,]\,. \tag{3.4}$$

Consistent boundary conditions are then

$$\text{on } x = 0\,,\quad \begin{matrix} T_x = -\dfrac{12VL}{H^3}\,y \\ T_y = -\dfrac{3V}{2H^3}\,(4y^2 - H^2) \end{matrix} \qquad \text{on } x = L\,,\quad \begin{matrix} T_x = 0 \\ T_y = \dfrac{3V}{2H^3}\,(4y^2 - H^2) \end{matrix}$$
$$\text{and on } y = \pm\frac{H}{2}\,,\quad \begin{matrix} T_x = 0 \\ T_y = 0 \end{matrix} \tag{3.5}$$

along with the conditions $u_x(0,0) = u_y(0,0) = 0$ and $u_x(0, H/2) = 0$.

4. Analytical Example in Polar Coordinates

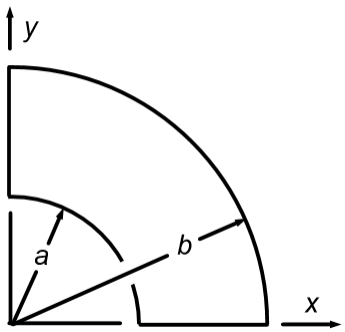

Figure 2. Quarter-annular domain.

In polar coordinates, the quarter-annular domain shown at left in Fig. 2 is subjected to the boundary conditions

$$u_r(a,\theta) = u_\theta(a,\theta) = 0\,,$$
$$T_r(b,\theta) = \frac{2F}{b}\cos 4\theta\,, \qquad T_\theta(b,\theta) = 0\,,$$
$$T_r(r,0) = 0\,, \qquad u_\theta(r,0) = 0\,, \tag{4.1}$$
$$T_r(r,\pi/2) = 0\,, \qquad u_\theta(r,\pi/2) = 0\,,$$

where

$$F = \int_0^{\pi/8} T_r(b,\theta)\, b\,\mathrm{d}\theta\,. \tag{4.2}$$

The boundary conditions (4.1) may be satisfied with a displacement field of the form

$$u_r = f(r)\cos 4\theta\,, \qquad u_\theta = g(r)\sin 4\theta\,. \tag{4.3}$$

Substituting eqns. (4.3) into the strain-displacement relations (1.9), one obtains the strains

$$\varepsilon_{rr} = f'\cos 4\theta\,, \qquad \varepsilon_{\theta\theta} = \frac{1}{r}(f + 4g)\cos 4\theta\,, \qquad \varepsilon_{r\theta} = \frac{1}{2}\left(g' - \frac{1}{r}g - \frac{4}{r}f\right)\sin 4\theta\,, \tag{4.4}$$

and via Hooke's Law (1.3), eqns. (4.4) give the stresses

$$\sigma_{rr} = \frac{1}{C(1-2\nu^*)}\left[(1-\nu^*)f' + \frac{\nu^*}{r}f + \frac{4\nu^*}{r}g\right]\cos 4\theta\,,$$
$$\sigma_{\theta\theta} = \frac{1}{C(1-2\nu^*)}\left[\nu^* f' + \frac{(1-\nu^*)}{r}f + \frac{4(1-\nu^*)}{r}g\right]\cos 4\theta\,, \tag{4.5}$$

$$\sigma_{r\theta} = \frac{1}{2C}\left(g' - \frac{1}{r}g - \frac{4}{r}f \right)\sin 4\theta \,.$$

Note that eqns. (4.3) and (4.5) satisfy the boundary conditions at $\theta = 0$ and $\theta = \pi/2$ identically. Now, substitution of the stresses (4.5) into the equilibrium eqns. (1.8) yields the coupled pair of ordinary differential equations

$$(1-\nu^*)f'' + \frac{(1-\nu^*)}{r}f' - \frac{(9-17\nu^*)}{r^2}f + \frac{2}{r}g' - \frac{2(3-4\nu^*)}{r^2}g = 0\,,$$
$$(1-2\nu^*)g'' + \frac{(1-2\nu^*)}{r}g' - \frac{(33-34\nu^*)}{r^2}g - \frac{4}{r}f' - \frac{4(3-4\nu^*)}{r^2}f = 0\,. \qquad (4.6)$$

By assuming functions of the form

$$f = kr^p\,, \qquad g = lr^p\,, \qquad (4.7)$$

eqns. (4.6) become

$$\begin{bmatrix} [\,(1-\nu^*)p^2 - (9-17\nu^*)\,] & 2[\,p-(3-4\nu^*)\,] \\ -4[\,p+(3-4\nu^*)\,] & [\,(1-2\nu^*)p-(33-34\nu^*)\,] \end{bmatrix}\begin{bmatrix} k \\ l \end{bmatrix} = \begin{bmatrix} 0 \\ 0 \end{bmatrix}, \qquad (4.8)$$

which has nontrivial solutions if the determinant of coefficients is zero, *viz.,*

$$p^4 - 34p^2 + 225 = 0\,. \qquad (4.9)$$

Thus,

$$p = -5\,,-3\,,3\,,5\,. \qquad (4.10)$$

Next, using the four null vectors of eqns. (4.8) as generated by the powers (4.10), one obtains the relations between the eight constants k_i and l_i

$$p=-5 \;\Rightarrow\; l_1 = k_1\,, \qquad p=-3 \;\Rightarrow\; l_2 = \frac{2\nu^*}{3-2\nu^*}k_2\,,$$
$$p=3 \;\Rightarrow\; l_3 = -k_3\,, \qquad p=5 \;\Rightarrow\; l_4 = -\frac{2(2-\nu^*)}{1+2\nu^*}k_4\,. \qquad (4.11)$$

Finally, the functions f and g are then

$$f = \frac{k_1}{r^5} + \frac{k_2}{r^3} + k_3 r^3 + k_4 r^5\,, \qquad g = \frac{l_1}{r^5} + \frac{l_2}{r^3} + l_3 r^3 + l_4 r^5\,. \qquad (4.12)$$

Turning attention to the boundary conditions at $r = a$ and $r = b$, eqns. (4.3), (4.5), (4.11) and (4.12) give the system

$$\begin{bmatrix} 1/a^5 & 1/a^3 & a^3 & a^5 \\ 1/a^5 & 2\nu^*/[\,(3-2\nu^*)a^3\,] & -a^3 & -2(2-\nu^*)a^5/(1+2\nu^*) \\ -5/b^5 & -9/[\,(3-2\nu^*)b^3\,] & 3b^3 & 5b^5/(1+2\nu^*) \\ -5/b^5 & -6/[\,(3-2\nu^*)b^3\,] & -3b^3 & -10b^5/(1+2\nu^*) \end{bmatrix}\begin{bmatrix} k_1 \\ k_2 \\ k_3 \\ k_4 \end{bmatrix} = \begin{bmatrix} 0 \\ 0 \\ 2FC \\ 0 \end{bmatrix} \qquad (4.13)$$

to solve for the constants k_i. The first of eqns. (4.13) is from $u_r(a,\theta) = 0$; the second is from $u_\theta(a,\theta) = 0$; the third, from $T_r(b,\theta) = 2F\cos 4\theta/b$; and the fourth, $T_\theta(b,\theta) = 0$. Instead of solving eqns. (4.13) algebraically, they were solved numerically using the constants

$$E = 3\times 10^7 \text{ psi}\,, \quad \nu = 0.3\,, \quad a = 36 \text{ in}\,, \quad b = 72 \text{ in}\,, \quad F = 10{,}000 \text{ lb} \qquad (4.14)$$

for plane stress. The results are

$$\begin{aligned} k_1 &= \ \ 4.468\,854\,986\,101\,9630 \times 10^{3} & l_1 &= \ \ 4.468\,854\,986\,101\,9630 \times 10^{3} \\ k_2 &= -6.240\,733\,337\,857\,3010 \times 10^{0} & l_2 &= -1.134\,678\,788\,701\,3274 \times 10^{0} \\ k_3 &= \ \ 1.437\,736\,140\,089\,1819 \times 10^{-9} & l_3 &= -1.437\,736\,140\,089\,1819 \times 10^{-9} \\ k_4 &= -1.194\,905\,134\,758\,0960 \times 10^{-13} & l_4 &= \ \ 2.892\,928\,220\,993\,2855 \times 10^{-13} \end{aligned} \quad , \tag{4.15}$$

which constants solve the problem at hand.

5. The 9–Noded Isoparametric Element

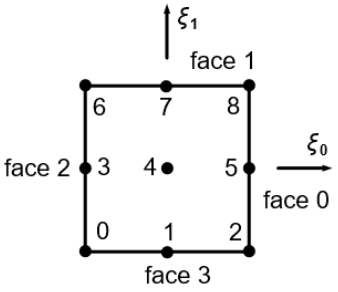

Figure 3. The element in **ξ**–space as described in the text.

At left, in Fig. 3, is pictured the element in normalized **ξ**–space, where $\xi_i \in (-1,1)$. The mapping to physical **x**–space is accomplished with

$$x_i = S^I x_i^I \ , \tag{5.1}$$

where x_i^I are the coordinates of the nodes in **x**–space. With the aid of the quadratic functions

$$a^0 = \frac{1}{2}(-\xi + \xi^2) \ , \quad a^1 = 1 - \xi^2 \ , \quad a^2 = \frac{1}{2}(\xi + \xi^2) \ , \tag{5.2}$$

the nine shape functions S^I are given by the tensor product

$$\begin{aligned} &S^0 = a^0(\xi_0)a^0(\xi_1) \ , && S^1 = a^1(\xi_0)a^0(\xi_1) \ , && S^2 = a^2(\xi_0)a^0(\xi_1) \ , \\ &S^3 = a^0(\xi_0)a^1(\xi_1) \ , && S^4 = a^1(\xi_0)a^1(\xi_1) \ , && S^5 = a^2(\xi_0)a^1(\xi_1) \ , \\ &S^6 = a^0(\xi_0)a^2(\xi_1) \ , && S^7 = a^1(\xi_0)a^2(\xi_1) \ , && S^8 = a^2(\xi_0)a^2(\xi_1) \ . \end{aligned} \tag{5.3}$$

Consistent with eqns. (5.1),

$$\frac{\partial x_i}{\partial \xi_\alpha} \equiv A_{i\alpha} = S^I_{,\alpha} x_i^I \ , \qquad \mathrm{d}x_i = A_{i\alpha}\,\mathrm{d}\xi_\alpha \ , \qquad \mathrm{d}\xi_\alpha = A^{-1}_{\alpha i}\,\mathrm{d}x_i \ , \qquad S^I_{,i} = S^I_{,\alpha} A^{-1}_{\alpha i} \ . \tag{5.4}$$

From the second of eqns. (5.4), integrals over the domain A may be transformed as

$$\int_{A^{\mathrm{x}}} (\ )\ \mathrm{d}A^{\mathrm{x}} = \int_{A^{\xi}} (\ )(\det \mathbf{A})\ \mathrm{d}A^{\xi} \ , \tag{5.5}$$

where $\mathrm{d}A^{\mathrm{x}}$ is the differential of area in **x**–space, and $\mathrm{d}A^{\xi}$ is the differential of area in **ξ**–space. For integrals along the boundary, $\mathrm{d}x_i = A_{i0}\,\mathrm{d}\xi_0$ (on faces1 and 3, *cf.,* Fig. 3, where $\mathrm{d}\xi_1 = 0$) and $\mathrm{d}x_i = A_{i1}\,\mathrm{d}\xi_1$ (on faces 0 and 2 where $\mathrm{d}\xi_0 = 0$). Thus, $(\mathrm{d}t)^2 = \mathrm{d}x_i \mathrm{d}x_i$ implies

$$\begin{aligned} \oint_t (\ )\,\mathrm{d}t &= \int_{-1}^{1} (\ )\sqrt{A_{i0}A_{i0}}\ \mathrm{d}\xi_0 \ \ \text{(faces 1 and 3)} \ , \\ \oint_t (\ )\,\mathrm{d}t &= \int_{-1}^{1} (\ )\sqrt{A_{i1}A_{i1}}\ \mathrm{d}\xi_1 \ \ \text{(faces 0 and 2)} \ . \end{aligned} \tag{5.6}$$

Numerically, the right-hand integrals in eqns. (5.5) and (5.6) are calculated with the three-point Gauss-Legendre quadrature rule, which rule integrates fifth order polynomials exactly.

Turning attention now to the Principle of Virtual Work, interpolate the virtual displacement u_j^* as

$$u_j^* = S^I u_j^{*I} \ , \qquad u_{j,i}^* = S_{,i}^I u_j^{*I} \ , \tag{5.7}$$

where u_j^{*I} are the nodal values of the virtual displacement u_j^*. Note that eqns. (5.1) and the first of eqns. (5.7) are of the same form. Hence the term "isoparametric". Nevertheless, substitution of eqns. (5.7) into the Principle of Virtual Work (2.4) gives

$$u_j^{*I} \int_A S_{,i}^I L_{ijkl} u_{l,k} \, \mathrm{d}A = u_j^{*I} \oint_t S^I T_j \, \mathrm{d}t \ , \tag{5.8}$$

or since u_j^{*I} is arbitrary,

$$\int_A S_{,i}^I L_{ijkl} u_{l,k} \, \mathrm{d}A = \oint_t S^I T_j \, \mathrm{d}t \ . \tag{5.9}$$

Now, interpolate u_l and $u_{l,k}$ within the element as

$$u_l = S^J u_l^J \ , \qquad u_{l,k} = S_{,k}^J u_l^J \ , \tag{5.10}$$

where u_l^J are the nodal values of the displacement u_l. Finally, putting the second of eqns. (5.10) into eqn. (5.9) gives the stiffness relation for the element

$$K_{jl}^{IJ} u_l^J = f_j^I \ , \tag{5.11}$$

where

$$K_{jl}^{IJ} = \int_A S_{,i}^I L_{ijkl} S_{,k}^J \, \mathrm{d}A \ , \qquad f_j^I = \oint_t S^I T_j \, \mathrm{d}t \ . \tag{5.12}$$

6. Numerical Example in Cartesian Coordinates

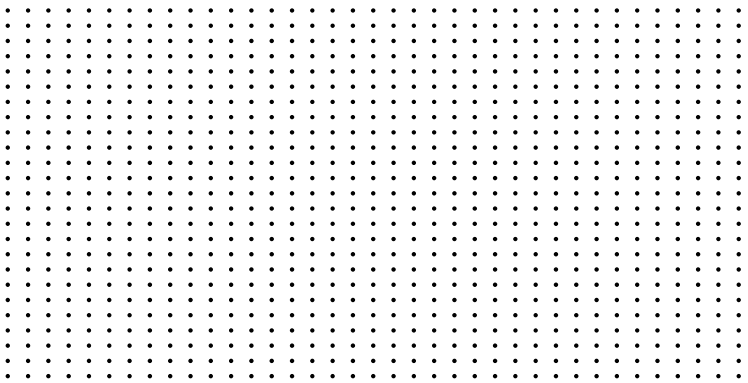

Figure 4. Grid used in the analysis as explained in the text.

Here the problem presented earlier in **§3** is analyzed numerically. The computational grid used is pictured above in Fig. 4. It consists of a 37×25 array of nodes, and an 18×12 array of elements. The constants used in the analysis are

$$E = 3.0 \times 10^7 \text{ psi} \ , \quad \nu = 0.3 \ , \quad V = 10000 \text{ lb/in} \ , \quad L = 10 \text{ in} \ , \quad H = 5 \text{ in} \ , \tag{6.1}$$

and plane stress is assumed.

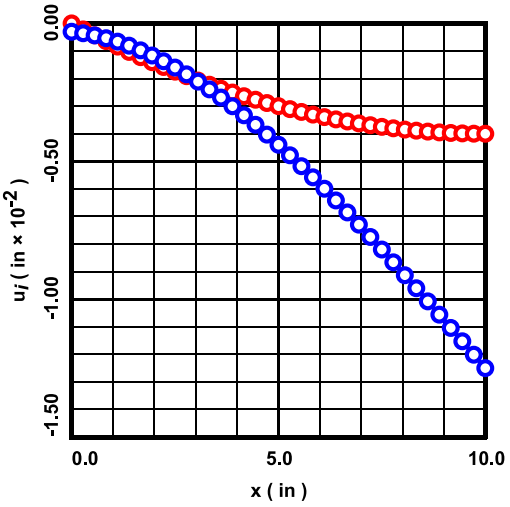

Figure 5. Displacement components u_x (red) and u_y (blue) at $y = -2.5$ in.

In all the graphs: the solid curves show the exact solution; and the plotted points, the numerical solution. For the numerical solution: the displacement components u_i are calculated at the nodes; the stress components σ_{ij} are also calculated at the nodes (by using the gradients of the element shape functions and nodal averaging).

Figure 5 at left shows the results for the displacement components u_i along the bottom of the domain at $y = -2.5$ in. As is evident, the numerical solution basically reproduces the exact solution.

Figures 6 and 7 below show the results at the left end of the domain $x = 0$. As is evident, once again, the numerically calculated displacements u_i (Fig. 6), and stress components σ_{xx} and σ_{xy} (Fig. 7), basically coincide with the exact solution.

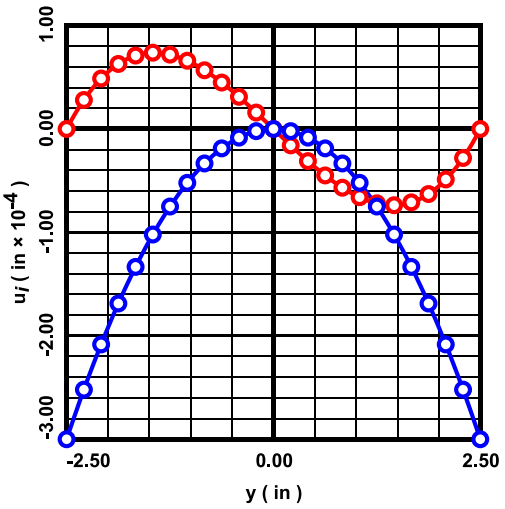

Figure 6. Displacement components u_x (red) and u_y (blue) at $x = 0$.

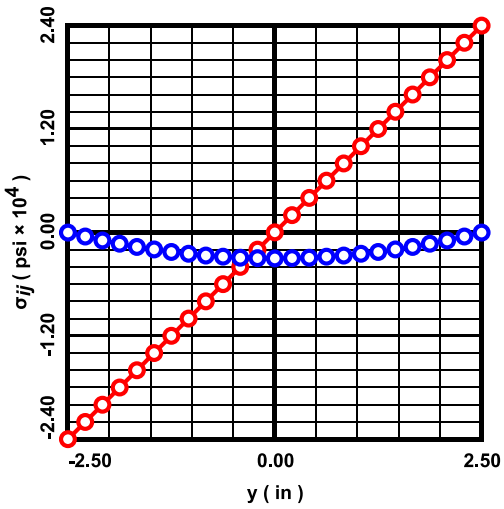

Figure 7. Stress components σ_{xx} (red) and σ_{xy} (blue) at $x = 0$.

Figures 8 and 9 below present the results along the right end of the domain located at $x = 10$ in. Here also, the numerically calculated displacement components u_i (Fig. 8), and stress component σ_{xy} (Fig. 9) are highly accurate.

Finally, Figs. 10 and 11 below give the results along a vertical line through the grid located at $x = 7.5$ in. As before, the numerical results for the displacement components u_i (Fig.10), and stress components σ_{xx} and σ_{xy} (Fig. 11), for all practical purposes, reproduce the exact solution.

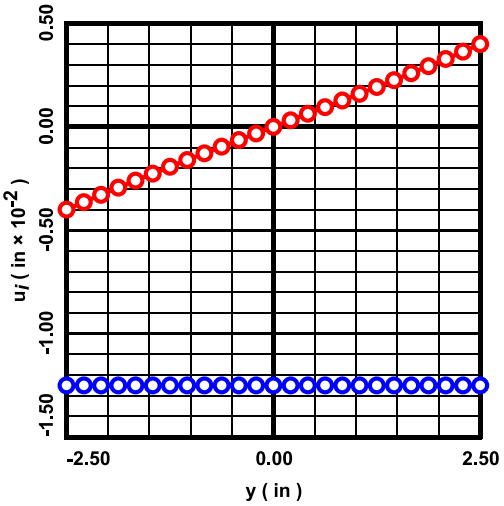

Figure 8. Displacement components u_x (red) and u_y (blue) at $x = 10$ in.

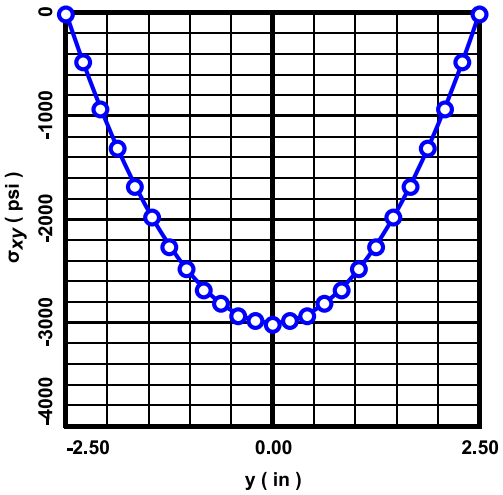

Figure 9. Stress component σ_{xy} at $x = 10$ in.

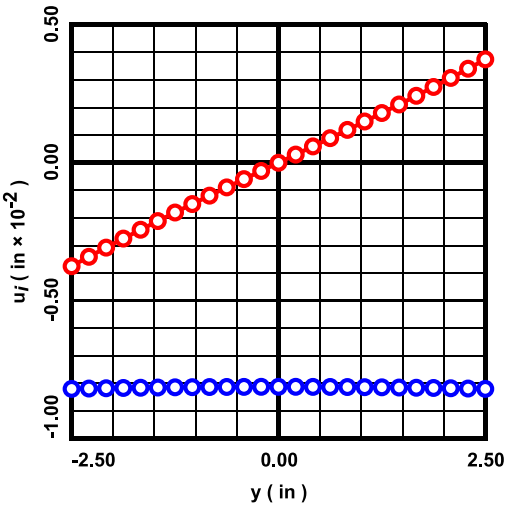

Figure 10. Displacement components u_x (red) and u_y (blue) at $x = 7.5$ in.

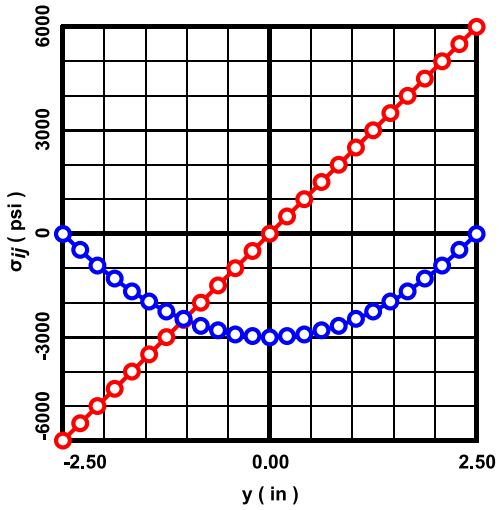

Figure 11. Stress components σ_{xx} (red) and σ_{xy} (blue) at $x = 7.5$ in.

7. Numerical Example in Polar Coordinates

The problem presented above in **§4** is solved here numerically. The computational grid used for the numerical analysis is shown below in Fig. 12. It consists of a 25 (radial) × 37 (tangential) array of nodes, and a 12 (radial) × 18 (tangential) array of elements. The constants used in the analysis were given previously in eqns. (4.14). Plane stress is assumed.

In all the graphs herein: the solid curves show the exact solution; and the plotted points, the numerical solution. For the numerical solution: the displacement components u_i are calculated at the nodes; the stress components σ_{ij} are also calculated at the nodes (by using the gradients of the element shape functions and nodal averaging).

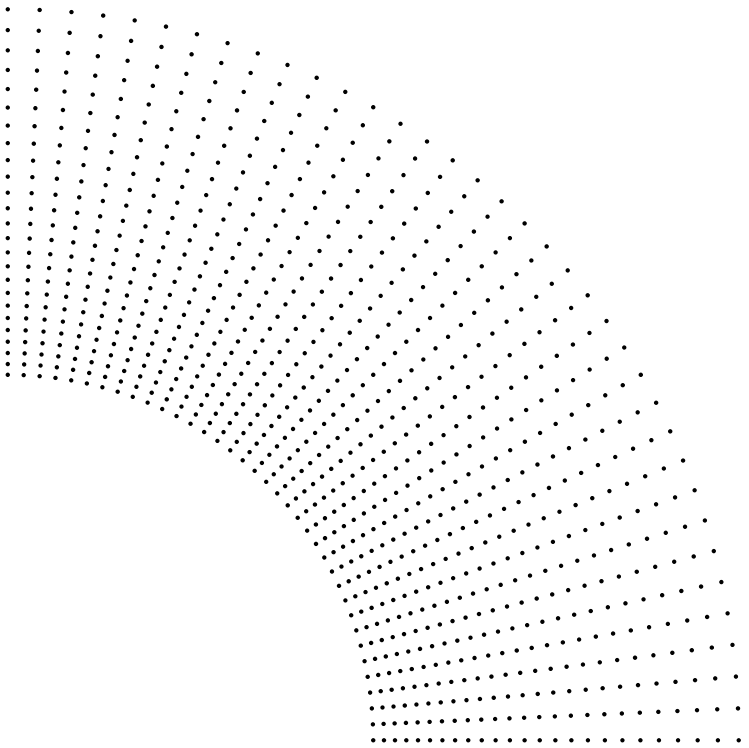

Figure 12. Computational grid used in the analysis as described in the text.

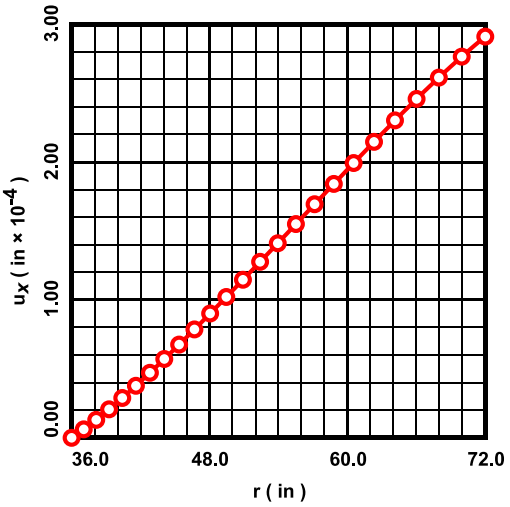

Figure 13. Displacement component u_x at $\theta = 0$.

Figure 13 at left presents the results for the displacement component u_x along the bottom of the domain at $\theta = 0$. Figure 14 below shows the results for the stress components σ_{xx} and σ_{yy} also at $\theta = 0$. As is seen from both the figures, the numerically calculated results are highly accurate.

Figures 15 and 16 depict the results at the outer radius of the domain $r = 72$ in. Figure 15 shows the numerically calculated displacements components u_x and u_y, which again, are very accurate. The stress components are shown in Fig. 16. Except for the minor inaccuracies in σ_{xx} near $\theta = \pi/2$, and in σ_{yy} near $\theta = 0$, the remaining numerical results are accurate.

Figure 17 below shows the results for the stress components σ_{xx}, σ_{yy} and σ_{xy} at the inner radius of the domain $r = 36$ in. In this case, all three numerically calculated stress components basically reproduce the exact solution.

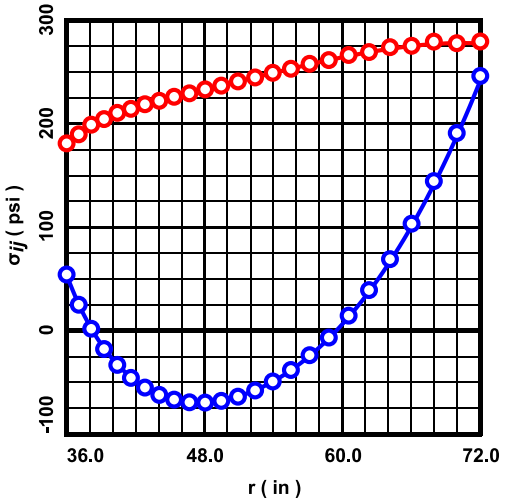

Figure 14. Stress components σ_{xx} (red) and σ_{yy} (blue) at $\theta = 0$.

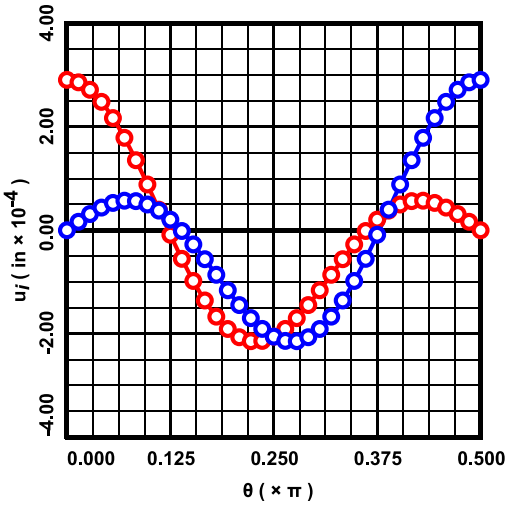

Figure 15. Displacement components u_x (red) and u_y (blue) at $r = 72$ in.

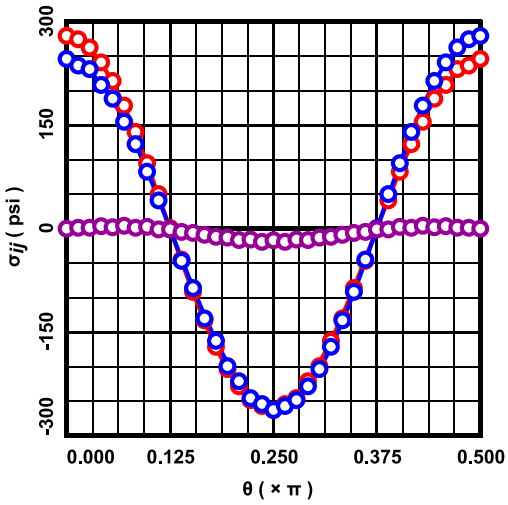

Figure 16. Stress components σ_{xx} (red), σ_{yy} (blue) and σ_{xy} (purple) at $r = 72$ in.

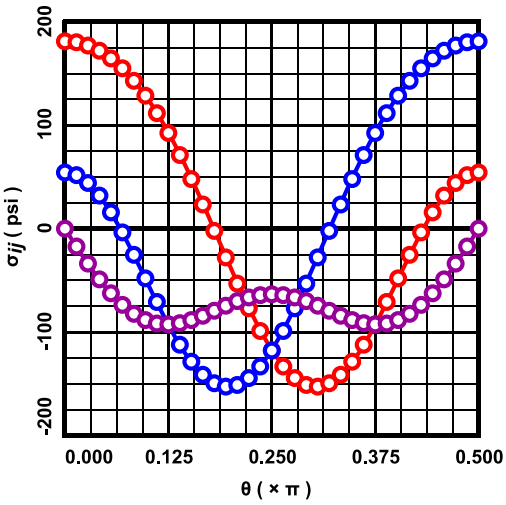

Figure 17. Stress components σ_{xx} (red), σ_{yy} (blue) and σ_{xy} (purple) at $r = 36$ in.

Figures 18 and 19 below present the results along a radial line through the grid located at $\theta = \pi/8$. As has been the case, the numerically calculated displacement components u_x and u_y basically coincide with the exact solution. For the stress components σ_{xx} and σ_{yy}, the numerically calculated results also are very accurate. Note that at $\theta = \pi/8$, $\sigma_{xy} = \sigma_{yy}$.

Finally, Figs. 20 and 21 below depict the results along a ring of nodes through the grid located at $r = 53.939$ in. Yet once again, the numerically calculated displacement components u_x and u_y (Fig. 20) and stress components σ_{xx}, σ_{yy} and σ_{xy} (Fig. 21) all are highly accurate.

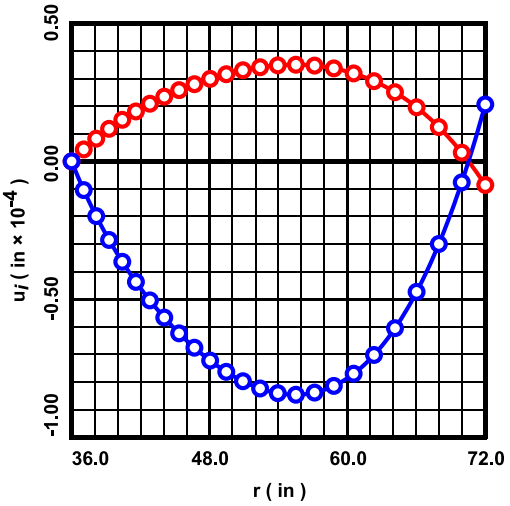

Figure 18. Displacement components u_x (red) and u_y (blue) at $\theta = \pi/8$.

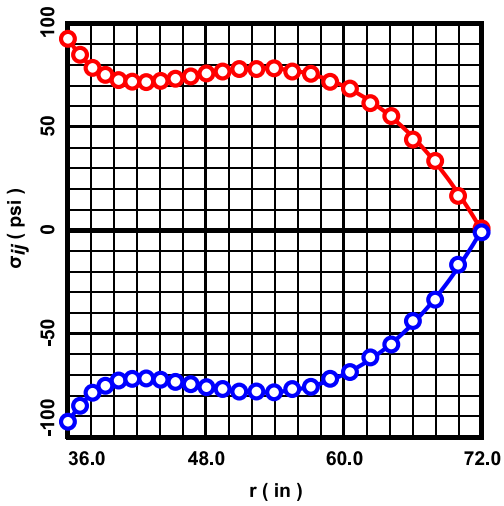

Figure 19. Stress components σ_{xx} (red) and σ_{yy} (blue) at $\theta = \pi/8$.

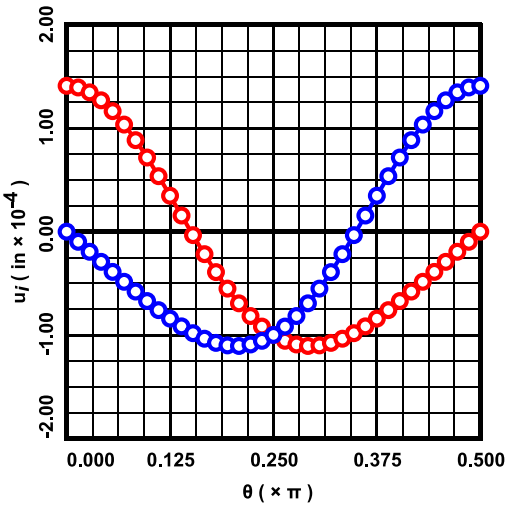

Figure 20. Displacement components u_x (red) and u_y (blue) at $r = 53.939$ in.

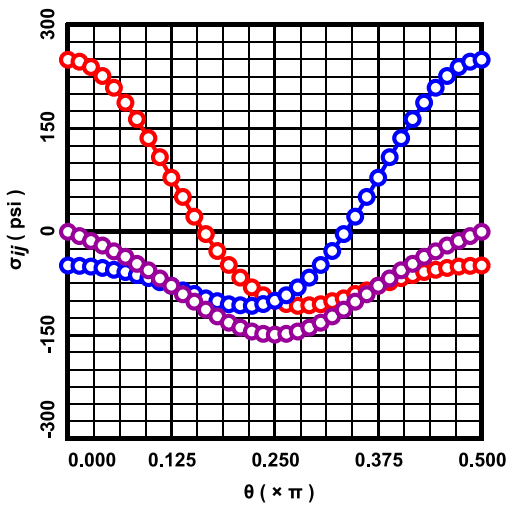

Figure 21. Stress components σ_{xx} (red), σ_{yy} (blue) and σ_{xy} (purple) at $r = 53.939$ in.

8. Closing Remarks

Obviously, the 9–noded isoparametric element of **§5** is both highly reliable and highly accurate, and it is the finite element of choice for two-dimensional linear elasticity. It is worth mentioning that if the grids of nodes in Figs. 4 and 12 are meshed with the 4–noded isoparametric element, then the numerical results obtained are significantly less accurate.